All atomic wave functions were generated by the method of Bursten, Jensen, and Fenske.[26] Contracted double-ζ representations were used for the Fe 3d, P 3p, and C 2p AO's. The hydrogen 1s AO utilized an exponent of 1.16.[27] The basis functions for Fe were derived for the +1 oxidation state with fixed 5s and 5p exponents of 2.0. The P basis functions were derived for the +0.45 oxidation state.

Summary

In order to study nucleophilic attack at internal carbons (C2/C4) of pentadienyl ligands, a family of electron-rich (η^5-pentadienyl)FeL_3^+ complexes has been synthesized. These complexes are obtained by treating (η^5-pentadienyl)$Fe(PEt_3)_2^+PF_6^-$ (**2**) with a series of 2e$^-$ donor ligands, L. In this paper, we report the synthesis of (η^5-pentadienyl)$Fe(PEt_3)_2(L)^+PF_6^-$ (L = CO, **3a**; L = $CNCMe_3$, **3b**), which are single rotamers (PEt_3 resides under the open pentadienyl mouth) and are chiral (the Fe atom is a stereogenic center).

Cations **3a** and **3b** undergo regioselective attack by alkyl anions at internal carbon C2 of the pentadienyl ligand. In particular, treatment of **3a,b** with methyllithium leads to the clean production of (2-methyl-1,3,4,5-η-pentenediyl)$Fe(PEt_3)_2(L)$ (L = CO, **4a**; L = $CNCMe_3$, **4b**), while treatment with *tert*-butyllithium generates (2-*tert*-butyl-1,3,4,5-η-pentenediyl)$Fe(PEt_3)_2(L)$ (L = CO, **5a**; L = $CNCMe_3$, **5b**). In each case, the $Fe(PEt_3)_2(L)^+$ fragment serves as an effective chiral auxiliary, directing diastereoselective addition to the less-hindered L-side of the pentadienyl ligand.

Work currently in progress is directed toward effecting further transformations of the pentenediyl ligands. Results of these studies will be reported in the future.

Acknowledgment. Support from the National Science Foundation (Grant CHE-8520680) is gratefully acknowledged. Washington University's X-ray Crystallographic Facility was funded by the National Science Foundation's Chemical Instrumentation Program (Grant CHE-8811456). The High Resolution NMR Service Facility was funded in part by the National Institutes of Health Biomedical Research Support Instrument Grant 1 S10 RR02004 and by a gift from the Monsanto Company. The Washington University Mass Spectrometry Resource is supported by a grant from the National Institutes of Health (RR00954).

Supplementary Material Available: Listings of final atomic coordinates, thermal parameters, bond lengths, bond angles, and significant least-squares planes for **2** and **5b** and an ORTEP drawing of the disordered PF_6^- group in **2**, showing all three sets of equatorial fluorine atoms (14 pages); listings of observed and calculated structure factor amplitudes (35 pages). Ordering information is given on any current masthead page.

(26) Bursten, B. E.; Jensen, J. R.; Fenske, R. F. *J. Chem. Phys.* **1978**, *68*, 3320.
(27) Hehre, W. J.; Stewart, R. F.; Pople, J. A. *J. Chem. Phys.* **1969**, *51*, 2657.

Bis(η^6-hexamethylbenzene)(η^6,η^6-[2_n]cyclophane)diruthenium-(II,II) Complexes and Their Two-Electron Reduction to [2_n]Cyclophane Derivatives Having Two Cyclohexadienyl Anion Decks Joined by an Extremely Long Carbon–Carbon Bond

Klaus-Dieter Plitzko,[1a] Brian Rapko,[1a] Bernhard Gollas,[1a] Gabriele Wehrle,[1a] Timothy Weakley,[1a] David T. Pierce,[1b] William E. Geiger, Jr.,*[,1b] Robert C. Haddon,*[,1c] and Virgil Boekelheide*[,1a,d]

Contribution from the Department of Chemistry, University of Oregon, Eugene, Oregon 97403, the Department of Chemistry, University of Vermont, Burlington, Vermont 05405, and AT&T Bell Laboratories, Murray Hill, New Jersey 07974. *Received January 8, 1990*

Abstract: A series of bis(η^6-hexamethylbenzene)(η^6,η^6-[2_n]cyclophane)diruthenium(II,II) tetrakis(tetrafluoroborate) complexes, **4**, **5**, **9**, **10**, and **11**, has been prepared, where the [2_n]cyclophanes are [2_2](1,4)cyclophane, [2_2](1,3)cyclophane, 4,7,13,16-tetramethyl-[2_2](1,4)cyclophane, 4,5,7,8-tetramethyl-[2_2](1,4)cyclophane, and [2_3](1,3,5)cyclophane, respectively. These 4+ diruthenium complexes undergo two-electron reduction to give **7**, **8**, **12**, **13**, and **14**, respectively, in which each of the cyclophane ligands now has two cyclohexadienyl anion decks connected by a new carbon–carbon bond. The assignment of structures to these two-electron reduction products is based on ^1H and ^{13}C NMR spectral analyses, electrochemical studies, and X-ray photoelectron data. A single-crystal X-ray analysis confirmed the structure assigned to the [2_2](1,4)cyclophane derivative **7** and showed that the carbon–carbon bond connecting the two cyclohexadienyl anion decks in **7** is 1.96 (3) Å in length, an extremely long carbon–carbon bond. A theoretical analysis of these 2+ diruthenium complexes and their formation is presented.

Recently we described a synthesis of bis(η^6-hexamethylbenzene)(η^6,η^6-[2_4](1,2,4,5)cyclophane)diruthenium(II,II) tetrakis(tetrafluoroborate), **1**, and its reduction to the corresponding 2+ ion, **2**, and the neutral species, **3**.[2] A study of the 2+ ion **2** showed it to be a mixed-valence ion (class II), exhibiting a net two-electron intervalence transfer. Although the ^1H and ^{13}C NMR spectra of **2** are symmetrical at room temperature, indicating the same environment for each of the two ruthenium atoms, cooling of these NMR solutions leads to a coalescence of signals and, below −45 °C, the two ruthenium atoms have different environments,

(1) (a) University of Oregon. (b) University of Vermont. (c) AT&T Bell Laboratories. (d) To whom inquiries regarding this manuscript should be addressed.

(2) Voegeli, R. H.; Kang, H. C.; Finke, R. G.; Boekelheide, V. *J. Am. Chem. Soc.* **1986**, *108*, 7010-7016.

0002-7863/90/1512-6545$02.50/0

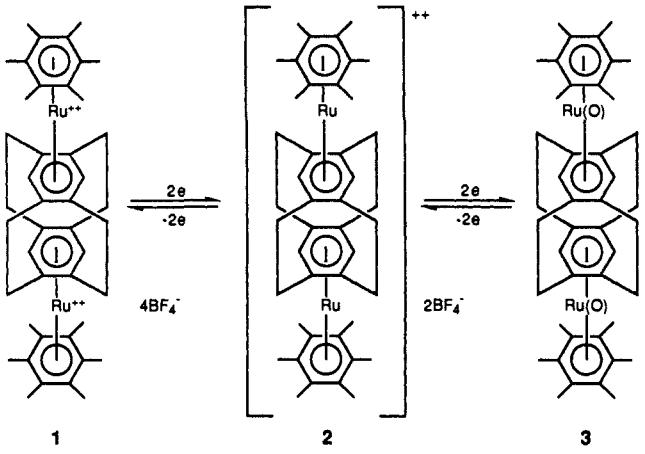

1 2 3

a ruthenium(II) site and a ruthenium(0) site. The interpretation of this behavior is given by the equilibrium between **2a** and **2b**, involving a two-electron intervalence transfer.

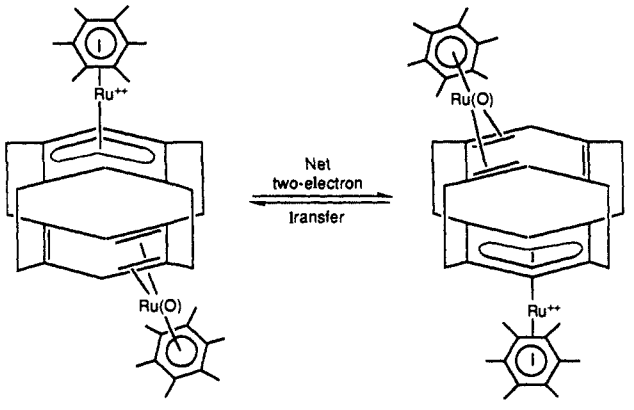

2a **2b**

The extension of this previous work to other examples of diruthenium(II,II) complexes of [2_n]cyclophanes was complicated by the unusual electrochemical behavior encountered with these further examples. The cyclic voltammograms of the known diruthenium cyclophane complexes, **4** and **5**, appeared most forbidding.[3] However, Bowyer and Geiger have shown that the unusually shaped cyclic voltammograms exhibited by Ir(III) and Ir(I) derivatives are due to slow charge transfer.[4a] Later, we encountered a similar behavior with bis(η^6-hexamethylbenzene)(η^6,η^6-9,10-dihydrophenanthrene)diruthenium(II,II) tetrakis(tetrafluoroborate), **6**, but the chemical reduction of **6** proceeded smoothly in high yield to give the corresponding 2+ diruthenium ion.[5]

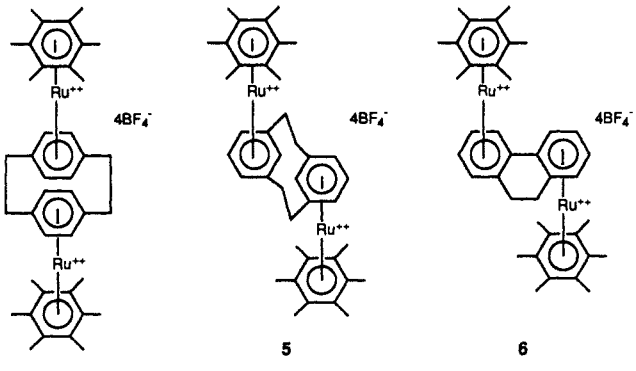

4 5 6

We have now explored the chemical reductions of **4** and **5**, and each of these 4+ diruthenium complexes are reduced, by using either cobaltocene or bis(hexamethylbenzene)ruthenium(0) as reagents, to give the corresponding dications, **7** and **8**, in high yield. To explore this behavior in greater depth we have also prepared the 4+ diruthenium complexes **9**, **10**, and **11**, and these likewise readily undergo chemical reduction to give their corresponding 2+ diruthenium complexes **12**, **13**, and **14**.

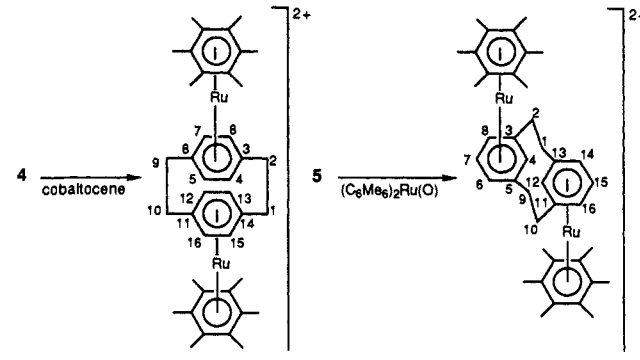

7 **8**

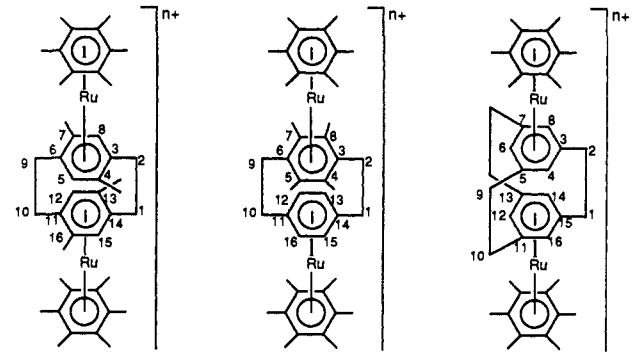

9, n = 4 **10**, n = 4 **11**, n = 4

12, n = 2 **13**, n = 2 **14**, n = 2

For purposes of comparison the 2+ monoruthenium complexes **15**, **16**, and **17** have been prepared. The other two 2+ monoruthenium complexes, **18** and **19**, were already available from previous work.[6]

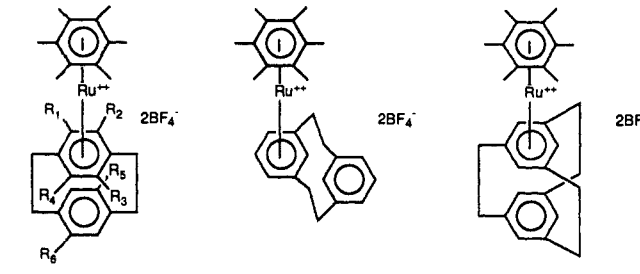

15, R_1-R_6 = -H
16, R_1, R_3, R_5, R_6 = -Me
R_2, R_4 = -H
17, R_1-R_4 = -Me
R_5, R_6 = -H

18 **19**

Structures of the 2+ Diruthenium-[2_n]Cyclophane Complexes. Examinations of the ^1H and ^{13}C NMR spectra of the 2+ diruthenium-[2_n]cyclophane complexes **7**, **8**, **12**, and **14** revealed that in each case the environment of the two ruthenium-bound hexamethylbenzene moieties is the same, i.e., the ^1H and ^{13}C NMR

(3) Swann, R. T.; Hanson, A. W.; Boekelheide, V. *J. Am. Chem. Soc.* **1986**, *108*, 3324-3334.

(4) (a) Bowyer, W. J.; Geiger, W. E. *J. Am. Chem. Soc.* **1985**, *107*, 5657-5663. (b) It should be noted that the behavior of these diruthenium complexes of [2_n]cyclophanes is quite different from that of the diiron complexes of [2_n]cyclophanes, see: Bowyer, W. J.; Geiger, W. E.; Boekelheide, V. *Organometallics* **1984**, *3*, 1079-1086.

(5) (a) Plitzko, K.-D.; Boekelheide, V. *Angew. Chem.* **1987**, *99*, 715-717; *Angew. Chem., Int. Ed. Engl.* **1987**, *26*, 700-702. (b) Plitzko, K.-D. Ph.D. Dissertation, University of Oregon, March 1987, pp 61-73.

(6) Laganis, E. D.; Voegeli, R.H.; Swann, R. T.; Finke, R. G.; Hopf, H.; Boekelheide, V. *Organometallics* **1982**, *1*, 1415-1420.

resonances show only one type of hexamethylbenzene. Furthermore, when solutions of these 2+ ions are cooled as low as is experimentally feasible (−100 to −120 °C), no change occurs in their ^1H or ^{13}C NMR spectra. This is in contrast to **2**, whose NMR spectra, although symmetrical at room temperature, change on cooling below −45 °C to show the characteristics of both a Ru(0) site and a Ru(II) site, as is typical for a mixed-valence ion (class II) having an appreciable energy barrier for intervalence electron transfer.

X-ray Photoelectron Spetra. Because the time scale for NMR measurements is relatively slow ($\sim 10^{-9}$ s), it seemed possible that these new 2+ diruthenium ions might be mixed-valence ions (class II), but ones having an energy barrier for intervalence electron transfer too small to be observed by NMR. Since the time scale for X-ray photoelectron spectroscopy is much faster (10^{-17} s), it seemed that X-ray photoelectron spectral data might be useful in exploring whether these 2+ diruthenium complexes have an energy barrier for intervalence electron transfer. The X-ray photoelectron spectrum of **2**, for example, shows two signals of 1:1 intensity at 280.8 and 282.0 eV for the binding energies of $Ru_{3d5/2}$.[2] This double signal is appropriate for the presence of a Ru(0) and a Ru(II) site as depicted by the equilibrium **2a** ⇌ **2b**. The X-ray photoelectron spectra of the 2+ diruthenium complexes **7**, **8**, **12**, **13**, and **14** are very similar to each other[7] but different from that of **2**.[2] Only one signal is observed for the binding energy of $Ru_{3d5/2}$, and this is nicely separated from the signal for C_{1s}. The experimental values for the $Ru_{3d5/2}$ binding energies are 281.8 eV for **7** and **8**, 281.3 eV for **12** and **14**, and 281.4 eV for **13**. These values, which so closely agree with each other, are only slightly lower than the value of 282.0 eV observed for the Ru(II) site of **2**.[2] Thus, the apparent conclusion from X-ray photoemission measurements is that there is only one type of ruthenium ion in all of these complexes, **7**, **8**, **12**, **13**, and **14**, and that it corresponds to a Ru(II) site attached to a ligand which is a somewhat better electron donor than the benzene decks of **2**.

However, the interpretation of X-ray photoelectron spectra of mixed-valence ions of transition-metal complexes is both difficult and not without ambiguity. The outstanding example typifying this is the Creutz–Taube ion, **20**.[8] Citrin observed two signals in the $Ru_{3d5/2}$ region of the X-ray photoelectron spectrum of **20**, which he assigned to separate Ru(II) and Ru(III) binding energies.[9] Subsequently, Hush pointed out that, theoretically, delocalized mixed-valence ions (class III) could also give rise to two photoemission signals of equal intensity.[10] After a careful reinvestigation of the X-ray photoelectron properties of **20**, Citrin and Ginsburg concluded that X-ray photoelectron spectroscopy fails to distinguish between a localized and delocalized ground-state for the Creutz–Taube ion, **20**.[11] Supposedly, a transition-metal complex having a ground state with a metal present in two different oxidation states might, through coincidence, show only a single signal. Thus, the conclusion that only one type of ruthenium site is present in **7**, **8**, **12**, **13**, and **14**, although highly likely, must still be regarded with some caution.

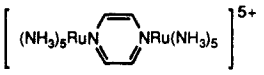

20

^1H and ^{13}C NMR Spectral Analysis of the 2+ Diruthenium–[2n]Cyclophane Complexes. As indicated previously, the ^1H and ^{13}C NMR chemical shift values for the hexamethylbenzene-ruthenium moieties present in **7**, **8**, **12**, and **14**, show that in each case both ruthenium environments are the same. The exception of **13**, which has an unsymmetrical methyl substitution pattern relative to the ruthenium atoms and so shows the expected small differences in the ^1H and ^{13}C values for the two different hexamethylbenzenes. However, the ^1H and ^{13}C NMR chemical shift patterns for the cyclophane ligands in **7**, **12**, **13**, and **14** are all unsymmetrical. Only in the case of the [2₂](1,3)cyclophane ligand present in **8** is the pattern of NMR signals symmetrical.

The unsymmetrical nature of these NMR spectra is typified by **7**, which shows a coupling between adjacent protons on the cyclophane deck (C4–H, δ 2.41, d, J = 5.7 Hz; C5–H, δ 4.43, d, J = 5.7 Hz). This pattern of a large chemical shift difference between adjacent aromatic protons prevails throughout the spectra of **7**, **8**, **12**, and **13**. In the case of **14**, there are no adjacent aromatic protons, but the ^1H NMR spectrum of **14** shows two types of aromatic protons which, by integration, are present in a 2:1 ratio (δ 4.56, s, 2 H; δ 3.38, s, 4 H). Table I summarizes the ^1H and ^{13}C NMR data for all these 2+ diruthenium–[2n]-cyclophane complexes. An analysis of the NMR chemical shift patterns summarized in Table I reveals a striking, but obvious, similarity of these patterns to those of the "open" metallocenes, studied so extensively by Ernst.[12] For example, the pattern of the ^{13}C NMR chemical shift values of the C-4, C-5, and C-6 carbons of the decks of **7** is quite similar to the corresponding pattern of the C-1, C-2, and C-3 carbons of the "open" ruthenocene **21**,[12c] as given in Table II. The patterns for the other cyclophane ligands present in complexes **8**, **12**, **13**, and **14** are also quite similar. Furthermore, the ^1H NMR chemical shift patterns of these cyclophane ligands are likewise in concurrence with that of the "open" ruthenocene **21**, to the extent that comparisons are possible. On the basis of this data the decks of the cyclophane ligands listed in Table I have been assigned "open" cyclohexadienyl anion structures.

Earlier we reported that the protonation of (η⁶-hexamethylbenzene)(η⁴-[2₂](1,4)cyclophane)ruthenium(0) gives **22**, the first example of a cyclophane containing a cyclohexadienyl anion deck, and the structure assigned to **22** has been established by a single-crystal X-ray analysis.[13] Here again the ^1H and ^{13}C chemical shift patterns of **22** are in agreement with those of **21** and the patterns of the cyclophane ligands of **7**, **8**, **12**, **13**, and **14**.

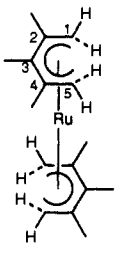

21

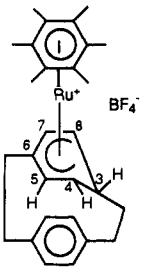

22

Since the position assignments made for the ^{13}C and ^1H NMR spectra of the cyclophane ligands of **7**, **8**, **12**, **13**, **14**, and **22** are arbitrary and were made, based in part, on an assumed relationship to the cyclohexadienyl anion models, it was important to obtain independent evidence that the assignments for the respective ^1H and ^{13}C NMR chemical shift values are internally consistent. This was examined by ^1H and ^{13}C NMR selective decoupling experiments for **7**, which established this correlation. For example, the

(7) We thank Dr. Gunter Barth and Surface Science Laboratories, Inc., Mountain View, CA, for making these X-ray photoelectron measurements. Binding energies are based on an internal reference sample of polypropylene (284.6 eV).

(8) Creutz, C.; Taube, H. *J. Am. Chem. Soc.* **1969**, *91*, 3988–3989; **1973**, *95*, 1086–1094.

(9) Citrin, P. H. *J. Am. Chem. Soc.* **1973**, *95*, 6472–6473.

(10) Hush, N. S. *Chem. Phys.* **1975**, *10*, 361.

(11) Citrin, P. H.; Ginsberg, A. P. *J. Am. Chem. Soc.* **1981**, *103*, 3673–3679.

(12) (a) Wilson, D. R.; DiLullo, A. A.; Ernst, R. D. *J. Am. Chem. Soc.* **1980**, *102*, 5928–5930. (b) Wilson, D. R.; Lui, J.-Z.; Ernst, R. D. *Ibid.* **1982**, *104*, 1120–1122. (c) Stahl, L.; Ernst, R. D. *Organometallics* **1983**, *2*, 1229–1234. (d) Böhm, M. C.; Eckert-Makric, M.; Ernst, R. D.; Wilson, D. R.; Gleiter, R. *J. Am. Chem. Soc.* **1982**, *104*, 2699–2707. (e) Gleiter, R.; Hyla-Kryspin, I.; Ziegle, M. L.; Sergeson, G.; Green, J. C.; Stahl, L.; Ernst, R. D. *Organometallics* **1989**, *8*, 298–306. (f) Ernst, R. D.; Melendez, E.; Arif, A. M.; Ziegler, M. L. *Angew. Chem.* **1988**, *100*, 1132–1134; *Angew. Chem., Int. Ed. Engl.* **1988**, *27*, 1099–1101.

(13) Swann, R. T.; Hanson, A. W.; Boekelheide, V. *J. Am. Chem. Soc.* **1986**, *108*, 3324–3334.

Table I. NMR Spectra of the 2+ Diruthenium Complexes[a,b]

compd	cyclophane ligand	^{1}H NMR chemical shift and J values											^{13}C NMR chemical shift values (position assignments)			
		ArCH	(position)	type	J	CH_2	(position)	type	J	CH_3	(position)	type	quaternary	tertiary	secondary	primary
7	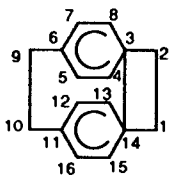	4.43	(5, 7, 12, 16)	d	5.7	2.95	(9, 10)	s		2.24	(HMB)[c]	s	110.3 (6, 11)	87.3 (5, 7, 12, 16)	28.3, 27.4 (1, 2, 9, 10)	17.6 (HMB-Me)[c]
		2.41	(4, 8, 13, 15)	d	5.7	1.87	(1, 2)	s					103.6 (HMB) 55.4 (3, 14)	45.9 (4, 8, 13, 15)		
12	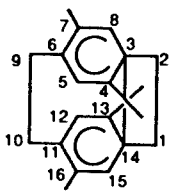	4.29	(5, 12)	s		3.2–2.8	(9, 10)	m		2.18	(HMB)[c]	s	109.5 (6, 11)	85.9 (5, 12)	24.5, 29.4 (1, 2, 9, 10)	16.8 (HMB-Me)[c]
		2.08	(8, 15)	s		2.3–2.0	(1, 2)	m		1.71	(7, 16)	s	102.9 (HMB)	46.6 (8, 15)		18.7, 18.4 (Me at 4, 13 & 7, 16)
										1.28	(4, 13)	s	94.9 (7, 16) 59.2 (4, 13) 55.8 (3, 14)			
13	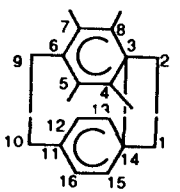	4.42	(12, 16)	d	6.0	3.2–2.9	(9, 10)	m		2.28	(HMB)[c]	s	109.5 (6, 11)	84.4 (12, 16)	28.1	17.3 (Me at 4,
		2.35	(13, 15)	d	6.0	2.2–1.7	(1, 2)	m		2.05	(HMB)[c]	s	104.6 103.5, 102.5 (HMB & HMB′) 93.7 (5, 7) 64.1 (4, 8) 54.0 (14) 51.2 (3)	44.4 (13, 15)	25.1, 24.4, 19.3 (1, 2, 9, 10)	17.2, 17.1, 16.1 5, 7, 8) (HMB-Me)[c]
8	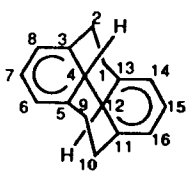	5.71	(7, 15)	t	4.8	2.02	(1, 2, 9, 10)	d	8.4	2.13	(HMB)[c]	s	99.3 (HMB)	87.0 (6, 8, 14, 16)	34.9 (1, 2, 9, 10)	16.7 (HMB-Me)[c]
		4.55	(6, 8, 14, 16)	d	4.8	1.50	(1, 2, 9, 10)	d	8.4				82.7 (3, 5, 11, 13)	70.2 (7, 15) 62.5 (4, 12)		
		2.41	(4, 12)	d												
14	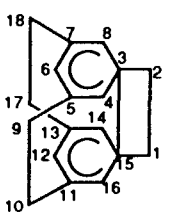	4.56	(6, 12)	s		2.06	(9, 10, 17, 18)	s		2.17	(HMB)[c]	s	100.4 (HMB)	89.0 (6, 12)	34.3, 30.1 (1, 2 and 9, 10, 17, 18)	17.2 (HMB-Me)[c]
		3.38	(4, 8, 14, 16)	s		1.73	(1, 2)	s					97.9 (5, 7, 11, 13) 78.3 (3, 15)	64.5 (4, 8, 14, 16)		

[a] All NMR spectra were measured with a QE-300 and/or a Nicolet NT-360 by using CD_2Cl_2 as solvent. [b] Chemical shift values (δ) are in reference to tetramethylsilane, and J values are in Hz. [c] HMB refers to hexamethylbenzene and HMB-Me to the methyl groups of hexamethylbenzene.

Table II. Comparison of ^1H and ^{13}C NMR Chemical Shift Patterns of **7** with **21** and **22**

compd	position assignments	^{13}C δ values	^1H δ values
7	C-4 and C-8	45.9	2.41
	C-5 and C-7	87.3	4.43
	C-6	110.3	
21	C-1 and C-5	48.4	2.84
	C-2 and C-4	95.5	
	C-3	105.3	
22	C-4 and C-8	55.1	2.90–2.87
	C-5 and C-7	91.8	4.08
	C-6	94.0	

protons of chemical shift value δ 2.41 are attached to the carbon of chemical shift value δ 45.9, and the protons, δ 4.43, are attached to the carbons, δ 87.3. Also, this correlation between ^1H and ^{13}C assignments was examined for our reference model **22** by application of the Attached Proton Test experiment, devised by Patt and Shoolery,[14] and is consistent with the assignment that the protons of **22**, δ 2.90–2.87, are attached to the carbons δ 55.1, and the protons, δ 4.08, are attached to carbons, δ 91.8. This provides good evidence that the position assignments for the ^1H and ^{13}C NMR spectra presented in Table I are indeed internally consistent.

There are several anomalies in Table I, though, and these are probably due to the fact that the magnitude of the upfield chemical shift which occurs, when transition metals are bonded to hydrocarbons, is reflected by geometric as well as electronic factors. It would be expected that the longer the Ru–C bond length the weaker the bond and the smaller the ^{13}C NMR upfield chemical shift due to transition-metal bonding. These differences in Ru–C bond lengths appear to be the source of the anomalies in the correlation of the ^{13}C NMR chemical shift values of our cyclophane derivatives with the "open" ruthenocene models **21** and **22**, as summarized in Tables I and II. For example, the [2$_2$](1,4)-cyclophane derivatives **7**, **12**, and **13** would all be expected to have similar geometries, and in each of these derivatives the ^{13}C chemical shift value assigned to C6 is about δ 110, which is at appreciably lower field than the ^{13}C values assigned to the corresponding carbons in the reference models **21** (δ 105.3) and **22** (δ 94.0). However, X-ray analysis of **22** shows that the Ru–C4, Ru–C5, and Ru–C6 bond lengths differ only slightly and are all about 2.18 Å in length (see ref 13, Supplementary Material), whereas an X-ray analysis of **7** (vide infra) shows the corresponding bond lengths to be Ru–C4 = 2.14, Ru–C5 = 2.22, and Ru–C6 = 2.42 Å. The much greater bond length of 2.42 Å for the Ru–C6 bond of **7**, as compared to the length of 2.18 Å for the Ru–C6 bond of **22**, would appear to be the principal reason why the ^{13}C NMR chemical shift value of C6 in **7** has a much lower field value (δ 110.3) than that of C6 (δ 94.0) in **22**. That the ^{13}C chemical shift for the corresponding carbon, C3, in **21** has an intermediate value (δ 105.3) is in accord with the fact that the Ru–C3 bond length is 2.258 Å,[12c] a distance intermediate between the Ru–C6 bond lengths present in **7** and in **22**.

Another anomaly is the large upfield shift exhibited by C7 and C15 in the ^{13}C NMR spectrum of the *anti*-[2$_2$](1,3)cyclophane derivative **8**. Although the C7 and C15 carbons of **8** would be expected to have a similar electronic environment to that of the C6 carbons of **7** and **22**, their chemical shift value, δ 7.02, is at much higher field. Since the C7 and C15 regions of *anti*-[2$_2$]-(1,3)cyclophanes are much more flexible than the C6 region of [2$_2$](1,4)cyclophanes, it is likely that the Ru–C7 bond distance is much shorter than the Ru–C6 bond distances in **7** and **22**.

The chemical behavior and NMR spectral properties of the 2+ diruthenium–cyclophane complexes **7**, **8**, **12**, **13**, and **14** strongly suggest that these complexes are diamagnetic and not paramagnetic species. For that reason the cyclophane ligands in Table I are illustrated with a carbon–carbon bond connecting the two cyclohexadienyl anion decks, the C3–C14 bond in the [2$_2$]-(1,4)cyclophane derivatives **7**, **12**, and **13**. Because of the constraints of the fairly rigid geometry of the [2$_2$](1,4)cyclophane moiety, its C3–C14 bond would necessarily be quite long and be expected to have a lot of sp^2 character. Actually, the ^{13}C NMR chemical shift values for the C3 and C14 carbons of **7** and **12** are δ 55.4 and 55.8, respectively. For **13**, C3 and C14 appear at 54.0 and 51.2. Thus, the ^{13}C NMR chemical shift values observed for these quaternary carbons are very much in the intermediate region between where sp^3 and sp^2 carbon chemical shifts are usually observed.

Crystal Structure Analysis of 7. Even though their spectral properties provide strong evidence for the presence of two cyclohexadienyl anion decks in the cyclophane ligands of the 2+ diruthenium complexes **7**, **8**, **12**, **13**, and **14**, it was highly desirable to obtain a single-crystal X-ray structural analysis of an example of these 2+ ions not only as direct experimental evidence regarding the assigned structure but also to know more about the geometry and the nature of the carbon–carbon bond connecting the two cyclohexadienyl anion decks. To obtain suitable crystals of any of these 2+ ions proved to be an exceedingly onerous and difficult task.

The eventual solution to this problem was adventitious. Reduction of **4**, by treatment with cobaltocene, followed by exchange of the counterion of **7** with tosylate anion led to crystals of X-ray quality, but with a composition corresponding to [(hexamethylbenzene)$_2$([2$_2$](1,4)cyclophane)diruthenium]$_2^{2+}$[$(C_5H_5)_2Co$]$^+$-$(C_7H_7SO_3)_5^-$.[15] Apparently, contamination of the solution used for recrystallization of **7** by an impurity of cobaltocenium ion provided the right environment for formation of a good crystal lattice. The ^1H NMR spectrum of a solution of these crystals shows clearly the presence of the bis(hexamethylbenzene)-([2$_2$](1,4)cyclophane)diruthenium ion, **7**, the cobaltocenium ion, and the tosylate anions.

The packing diagram of the unit cell for these crystals is shown in Figure 1. The positions of the two units of **7**, the two one-half units of cobaltocenium ion, and four tosylate anions are well defined. There are a number of peaks in the voids of the unit cell, and these are refined as half-atoms of carbon and are interpreted as belonging to the fifth tosylate anion, present as two half anions related by an inversion center and showing orientational disorder. Unfortunately, the disorder associated with the fifth tosylate anion has resulted in convergence at R = 0.084 and so has limited the overall precision of our X-ray measurements (see data in the Supplementary Material for additional details).

A computer projection of the structure of **7**, deduced from the X-ray data, is presented in Figure 2, together with a summary of some of the important interatomic and mean plane distances. The geometry of the cyclophane ligand, shown in Figure 2, is appreciably distorted from that of the free hydrocarbon, [2$_2$]-(1,4)cyclophane.[16] The cyclohexadienyl anion character predicted for the decks of **7** is obviously present. Although the decks in **7** are still boat-shaped, they are somewhat flattened and closer together than in [2$_2$](1,4)cyclophane itself. The C3–C14 bond connecting the two decks is 1.96 (3) Å in length, possibly the longest carbon-to-carbon bond length ever measured by X-ray analysis.[17] It is of interest to note that the distance for the C3–C14 bond length of 1.96 (3) Å is greater than the value of 1.89 Å, measured by X-ray analysis, for the nonbonded contact distance between the bridgehead carbons of bicyclo[1.1.1]pentane.[18] Although the nonbonded contact distance between the

(14) Patt, S. L.; Shoolery, J. N. *J. Magn. Reson.* **1982**, *46*, 535–539.

(15) Crystal data: $(C_{40}H_{52}Ru_2)(C_{10}H_{10}Co)_{0.5}(C_7H_7SO_3)_{2.5}$, $C_{62.5}H_{74.5}$-$Co_{0.5}Ru_2S_{2.5}O_{7.5}$, M = 1257.5, triclinic, $P\bar{1}$, a = 13.325 (3) Å, b = 25.554 (5), c = 9.225 (2) Å, α = 91.84 (3)°, β = 105.89 (2)°, τ = 80.68 (2)°, V = 2981 (2), A^3, Z = 2, d_{calc} = 1.401 g cm^{-3}, graphite-monochromated Mo Kα radiation, λ = 0.71069 Å, μ = 8.8 cm^{-1}.

(16) Hope, H.; Bernstein, J.; Trueblood, K. N. *Acta Crystallogr.* **1972**, *B28*, 1733–1743. [2$_2$](1,4)cyclophane is also known as [2.2]paracyclophane.

(17) Outstanding previous examples of long carbon–carbon bonds measured by X-ray analysis include the C1–C6 bond (1.836 (7) Å) of an 11-methano[10]annulene derivative (Bianchi, R.; Morosi, G.; Mugnoli, A.; Simonetta, M. *Acta Crystallogr.* **1973**, *B29*, 1196–1208) and the C9–C10 bond (1.77 (1) Å) of the photoisomer of bi(anthracene-9,10-dimethylene) (Ehrenberg, M. *Acta Crystallogr.* **1966**, *20*, 182–186).

(18) Padwa, A.; Shefter, E.; Alexander, E. *J. Am. Chem. Soc.* **1968**, *90*, 3717–3721.

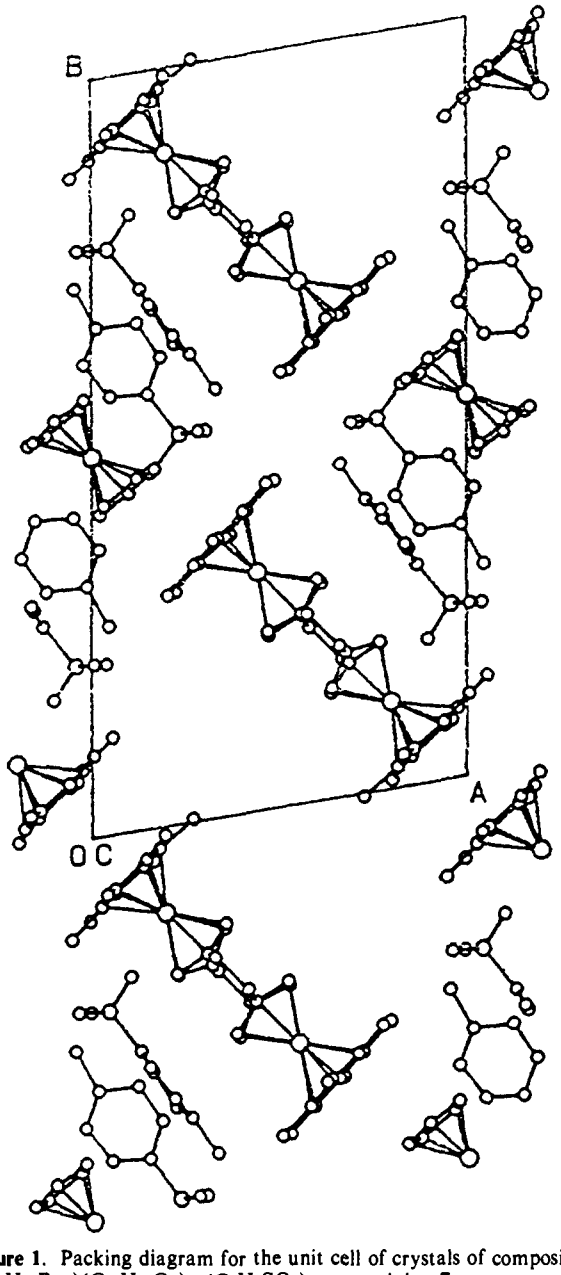

Figure 1. Packing diagram for the unit cell of crystals of composition, $(C_{40}H_{52}Ru_2)(C_{10}H_{10}Co)_{0.5}(C_7H_7SO_3)_{2.5}$, containing **7**.

C6 and C11 carbons of **7** is only 2.29 (3) Å, much shorter than the corresponding distance of 2.78 Å in $[2_2](1,4)$cyclophane itself, it is not truly exceptional as a short nonbonded contact distance. The length of the carbon–carbon bond (C9–C10) of the bridging methylenes in **7** is normal (1.53 (3) Å), as is the C1–C2 bond (1.55 (3) Å) of the cyclobutane ring. Similarly, the distance between the ruthenium atom and the mean plane of the hexmethylbenzene ring is 1.72 (3) Å and that between ruthenium and the mean plane of carbons C4, C5, C7, and C8 is 1.70 (3) Å, both quite usual distances. However, the Ru1–C6 bond length is 2.42 (3) Å, a much longer distance than Ru1–C5 (2.19 (2) Å) or Ru1–C4 (2.17 (2) Å). The structure of **7**, deduced from X-ray analysis, when combined with the spectral information showing a close analogy between **7** and the other 2+ diruthenium cyclophane complexes, plus the overall evidence that all of these cyclophane ligands have cyclohexadienyl anion decks, allows them an assignment of structure to **8**, **12**, **13**, and **14**, as shown below.

Of particular interest in all four structures, **8**, **12**, **13**, and **14**, is the carbon–carbon bond connecting the two cyclohexadenyl anion decks. In the case of **7**, this bond (C3–C14) is extremely long, being 1.96 (3) Å in length. Since **12** and **13** have the same skeletal framework as **7**, it would be expected that the C3–C14 bonds joining their cyclohexadienyl anion decks would be very

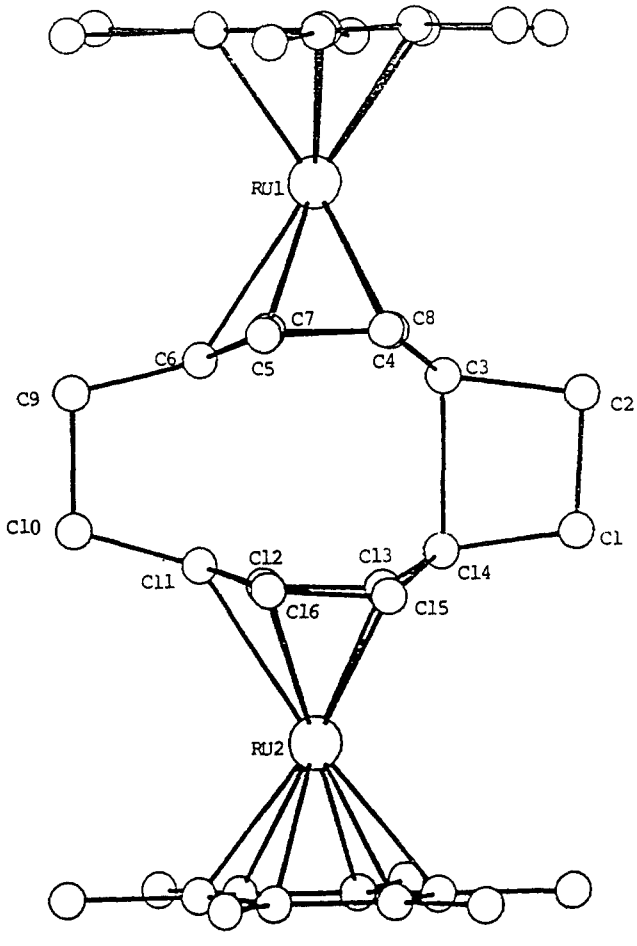

Important Interatomic and Mean Plan Distances Å

C1-C2	1.55(3)	C4-C5	1.39(3)
C9-C10	1.54(3)	C5-C6	1.56(4)
C3-C14	1.96(3)	Ru1-C4	2.22(2)
C6-C11	2.29(3)	Ru1-C5	2.14(2)
C2-C3	1.52(3)	Ru1-C6	2.42(3)
C3-C4	1.44(3)	Ru1-C8	2.17(2)

Ru1-Hexamethylbenzene (mean plane)	1.72(3)
Ru1-C4, C5, C7, C8 (mean plane)	1.70(3)

Figure 2. Computer projection of the structure of **7** as determined by X-ray analysis.

similar in length and their overall geometry would be quite analogous to that of **7**. For the *anti*-$[2_2](1,3)$cyclophane derivative **8**, though, there should be significant differences. It is well-known that *anti*-$[2_2](1,3)$cyclophanes readily undergo C4–C12 bond formation during chemical reactions, such as oxidation[19] or electrophilic substitution.[20] Thus, C4–C12 bond formation should be an easy process in the case of **8**, and the C4–C12 bond length in **8** should be in the normal range for an sp^3–sp^3 bond. On the other hand, the skeletal structure of $[2_3](1,3,5)$cyclophane is much more rigid than that of $[2_2](1,4)$cyclophane. Even though the distance between C3 and C15 in $[2_3](1,3,5)$cyclophane, as the free hydrocarbons, is 2.75 Å,[21] slightly shorter than the 2.78 Å distance between C3 and C14 in free $[2_2](1,4)$cyclophane,[16] further distortion of $[2_3](1,3,5)$to accommodate C3–C15 bond formation, as in **14**, would be expected to generate much more steric strain than is true for generating the C3–C14 bond in **7**. A reasonable

(19) Boekelheide, V.; Phillips, J. B. *J. Am. Chem. Soc.* **1967**, *89*, 1695–1704.
(20) Allinger, N. L.; Da Rooge, M. A.; Hermann, R. B. *J. Am. Chem. Soc.* **1961**, *83*, 1974–1978.
(21) Hanson, A. W. *Cryst. Struct. Comm.* **1980**, *9*, 1243–1248.

Table III. Cyclic Voltammetry Data for the 4+ Diruthenium Cyclophane Complexes **4** and **5**[a,b]

compd	ν, V s^{-1}	$E_{1/2}$, V	$E_{p,c}$, V	ΔE_p, mV	$E_p - E_{p/2}$, mV	$i_p/C\nu^{1/2}$	$E_{1/2}$, V	$E_{p,c}$, V	ΔE_p, mV	$E_p - E_{p/2}$, mV	$i_p/C\nu^{1/2}$
					A. Platinum Electrode						
4	1.0	−0.411	−0.44	57	38	0.85	−0.662	−0.77	219	62	0.50
	2.0	−0.405	−0.45	89	44	0.84	−0.669	−0.77	204	53	0.58
	5.0	−0.400	−0.45	117	47	0.86	−0.658	−0.77	233	45	0.74
5	1.0	−0.449	−0.47	39	34	2.5	−0.801	−0.82	42	32	0.78
	2.0	−0.453	−0.47	40	33	2.6	−0.805	−0.82	42	32	1.2
	5.0	−0.459	−0.48	42	40	2.6	−0.807	−0.83	47	35	1.6
					B. Mercury Electrode						
5	1.0	−0.449	−0.48	37	33	12	−0.798	−0.81	32	28	4.0
	2.0	−0.450	−0.48	39	37	13	−0.796	−0.81	36	31	5.7
	5.0	−0.450	−0.48	46	38	13	−0.796	−0.82	49	36	8.6

[a] **4** and **5** were measured in acetone containing 0.1 M n-Bu_4NPF_6 as electrolyte; redox potentials are vs SCE; **4** was measured at 233 K and **5** at 298 K. [b] ν = scan rate; V = volts; $E_{1/2}$ = average potential of cathodic ($E_{p,c}$) and ($E_{p,a}$) peaks; ΔE_p = potential separation between directly coupled anodic and cathodic peaks; $E_{p/2}$ = potential at one-half i_p; $i_p/C\nu^{1/2}$ = current function; i_a/i_c = ratio of anodic to cathodic peak currents.

prediction is that the C3–C15 bond in **14** is longer than 1.96 Å, the bond length found for the C3–C14 bond in **7**.

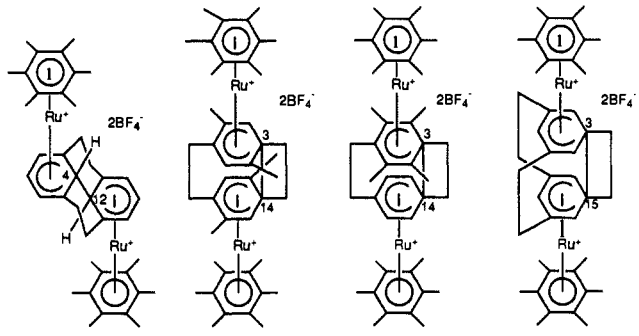

8 **12** **13** **14**

Electrochemical Studies. As indicated earlier, the cyclic voltammetry of the 4+ diruthenium complexes **4** and **5**[3] as well as the new examples **9**, **10**, and **11** is complicated by the appearance of broad waves, wide separation between peaks for the 4+/2+ couple, and limited chemical stability of the initial dications in polar solvents. To try to resolve these difficulties cyclic voltammetry of **4** and **15** in acetone was measured varying the nature of the electrode, the temperature, and the sweep rate. The resulting electrochemical data, summarized in Table III, shows that the first two-electron reduction in each case is followed by a chemically irreversible process. These irreversible chemical processes can be outrun at low temperatures and/or high potential sweep rates. In the case of **5**, as shown in Figure 3a, scanning at a sweep rate of less than 1 V s^{-1} gives a cyclic voltammogram showing two chemically irreversible cathodic peaks at about $E_{p,c}$ = −0.46 and −1.57 V (potential versus SCE) as well as partially reversible reductions at $E_{1/2}$ = −0.76 and $E'_{1/2}$ = −1.28 V. At a sweep rate of 50 V s^{-1} (Figure 3b), there are two reversible two-electron reductions at $E_{1/2}$ = −0.46 and $E'_{1/2}$ = −0.81 V with nearly equivalent current functions ($i_p/\nu^{1/2}$ = 5.8 μAs$^{1/2}$ V$^{1/2}$ and $i_p/\nu^{1/2}$ = 5.4 μAs$^{1/2}$ V$^{1/2}$).[22] Both electron transfers for **5** appeared to be fast at both platinum and mercury electrodes at sweep rates up to 5 V s^{-1}. Therefore, the two waves present in the high sweep rate voltammogram (Figure 3b) are reversible two-electron reduction waves in accord with eqs 1 and 2.

$$5^{4+} + 2e^- \rightleftharpoons 5^{2+} \quad (1)$$

$$5^{2+} + 2e^- \rightleftharpoons 5^0 \quad (2)$$

The sequence of the chemical (C) and electron transfer (E) steps governing the voltammograms of the diruthenium complex **5** are indicated by the peak currents for the observed 4+/2+ and 2+/0 couples. For a chemical step following the first reduction (an ECE process), and having a chemical reaction rate faster than the scan rate, the potential sweep is too slow to observe a wave for reduction of the dication. Conversely, the cathodic peak currents are nearly equal for both couples if the scan rate greatly exceeds the rate of the chemical reaction. Intermediate behavior, observed at moderate reaction or sweep rates, reflects a transition between these extreme kinetic regions and can be characterized by the ratio of cathodic peak currents for each redox step.

When the mechanism of the reduction of ECE, as given by eqs 3–5, the ratio of the cathodic current for the second wave (eq 5) to the first (eq 3) goes from 1.0 to 0 as the rate constant k_f of the intervening reaction (eq 4) increases. Thus, the measured ratio, $i_{c,2}/i_{c,1}$, at a particular sweep rate can be used to measure k_f. In the presence case, n = 2 for each wave.

$$A + ne^- \rightleftharpoons B \quad (3)$$

$$B \xrightarrow{k_f} Z \quad (4)$$

$$B + ne^- \rightleftharpoons C \quad (5)$$

This approach is similar to that described by Nicholson and Shain for an EM mechanism (eqs 3 and 4),[23] where the ECE

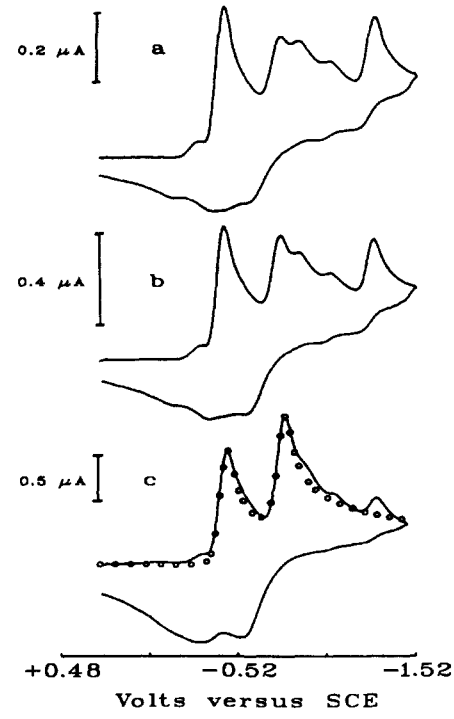

Figure 3. Cyclic voltammograms of 5^{4+}: (a) scan rate = 1 V s^{-1}; (b) scan rate = 50 V s^{-1} (solid line); (c) circles give the result of a theoretical simulation of two, Nernstein, two-electron transfers with $E_{1/2}$ = −0.48 V and −0.81 V versus SCE. Measurements made with solutions of 5^{4+} in acetone containing 0.1 M n-Bu_4NPF_6 by using a Pt disk electrode (r_o = 238 μm), concentration = 0.490 mM, and T = 298 K.

(22) The values in Table III and Figure 3 are given versus SCE to facilitate comparison with earlier papers in this series.

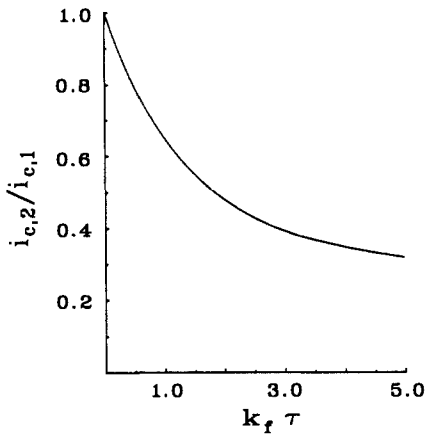

Figure 4. Theoretical plot of the current ratio for the two linear scan cathodic peaks of eqs 3 and 5 as a function of $k_f\tau$. k_f is the decomposition rate constant for the first electrode product (eq 4), and τ is the time in seconds necessary to scan from $E_{1/2}(1)$ to $E_{1/2}(2)$.

Table IV. Rate Constants (k_f) and Half-Lives ($t_{1/2}$) of the First-Order ECE Process Measured for the Diruthenium Complexes **4** and **5**[a-c]

compd	ν, V s^{-1}	$i_{p,c,2}/i_{p,c,1}$	k_f, s^{-1}	$t_{1/2}$, ms
4	1.0	0.58	5.58	124
	2.0	0.69	5.68	122
	5.0	0.87	5.81	119
5	1.0	0.32	14.2	49
	2.0	0.45	13.1	53
	5.0	0.62	14.4	48

[a] Measurements made by using a platinum electrode with solutions of **4** and **5** in acetone containing 0.1 M n-Bu_4NPF_6. **4** measured at 233 K and **5** at 298 K. [b] $i_{p,c,1}$ and $i_{p,c,2}$ are cathodic peak currents for the 4+/2+ and 2+/0 couples, respectively. [c] The rate constants were calculated from $i_{p,c,2}/i_{p,c,1}$ by using the working curve in Figure 4 from the formula $\tau = (E_{1/2},4^{+}/2+ - E_{1/2},2^{+}/0)/\nu$. The half-lives of the dications were calculated from the first-order rate constants.

current ratio ($i_{c,}2/i_{c,}1$) in our interpretation is analogous to their EC current ratio (i_a/i_c). Although a rate constant for the ECE mechanism can be measured from the i_a/i_c ratio (eq 3),[23] anodic peak currents are often perturbed by charging current at low temperatures and/or high sweep rates. Therefore, we developed a working curve which allows a rate analysis by using only cathodic currents. In Figure 4, a plot of cathodic peak current ratios versus the dimensionless rate parameter $k_f\tau$ has been constructed from the voltammograms simulating the reactions given by eqs 3–5 and compared to the experimental data measured for **5**. τ is the length of time taken in the scan between the $E_{1/2}$'s of the first and second waves. If only Nernstein voltammograms are considered, observed for **5** when the sweep rate is less than 10 V s^{-1}, peak current ratios for the $5^{4+}/5^{2+}$ and $5^{2+}/5^{0}$ couples were found to vary with sweep rate in a manner consistent with eqs 3–5. From the data presented in Table IV, the first-order rate constant, k_f, for **5** is calculated to be 13.9 ± 0.6 s^{-1}, giving an average half-life for 5^{2+} of 50 ± 2 ms. The nature of the irreversible chemical reaction was not ascertained, but is likely to involve the loss of a (hexamethylbenzene)ruthenium deck by solvolysis.

Cyclic voltammetry of 4^{4+} in acetone in temperatures above 253 K showed two major processes at potentials of about −0.40 and −1.30 V (potentials versus SCE), which were chemically irreversible even at very high scan rates. At 233 K, though, the diffusion-controlled $4^{4+}/4^{2+}$ couple at $E_{1/2}$ = −0.40 V (eq 6) began to show chemical reversibility, and a new reduction process corresponding to the $4^{2+}/4^{0}$ couple at $E_{1/2}$ = −0.66 V (eq 7) began to appear. These voltammograms are presented in Figure 5, where (a) corresponds to a scan rate of 1, (b) to 2, and (c) to 10 V s^{-1}. At higher sweep rates (Figure 5c), the current functions of both

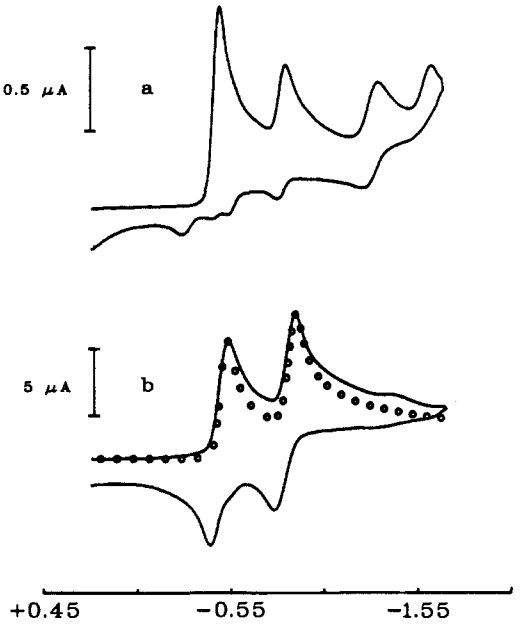

Figure 5. Cyclic voltammograms measured for a 0.457 mM solution of the 4^{4+} ion in acetone by using a Pt electrode at 233 K: (a) scan rate = 1 V s^{-1}; (b) scan rate = 2 V s^{-1}; (c) scan rate = 10 V s^{-1}; line = experimental values, whereas circles = values calculated from finite difference simulation of the EE process by using values given in the text.

reductions are nearly equal ($i_p/\nu^{1/2}$ = 0.84 $\mu As^{1/2}$ $V^{-1/2}$ for the first and $ip/\nu^{1/2}$ = 0.86 $\mu As^{1/2}$ $V^{-1/2}$ for the second), although the cathodic branch of the $4^{4+}/4^{2+}$ couple showed an $E_p - E_{p/2}$ value of 32 ± 4 mV, as expected for a nearly Nernstian two-electron process. The peak separation between cathodic and anodic processes (ΔE_p = 57 mV at 1.0 V s^{-1}) was indicative of a quasi-reversible charge transfer and/or a small contribution from uncompensated ohmic loss.[24]

$$4^{4+} + 2e^{-} \rightleftharpoons 4^{2+} \quad (6)$$

$$4^{2+} + 2e^{-} \rightleftharpoons 4^{0} \quad (7)$$

Characterization of the electrochemistry observed for 4^{4+} was hampered by the extreme conditions necessary to outrun the decomposition of 4^{2+} and by the slow charge transfer or ohmic losses exhibited by both redox steps under these conditions. However, an increase of the ratio of the $4^{2+}/4^{0}$ to $4^{4+}/4^{2+}$ cathodic peak currents to near unity at sweep rates greater than 1 V s^{-1} was strongly indicative of an irreversible chemical step following the first two-electron transfer process (see eqs 3–5). A first-order rate constant for the decomposition of 4^{2+} was calculated by using the working curve of Figure 4 and Table IV. A value of 5.7 ± 0.1 s^{-1} was obtained at 233 K, and a half-life of ca. 1 ms at room temperature was estimated for 4^{2+}.[25] These findings are supported by simulated voltammograms, which predict only a small wave for the $4^{2+}/4^{0}$ couple at room temperature.

From this electrochemical data it is apparent that the transient species, 4^{2+}, observed during cyclic voltammetry of 4^{4+}, is different from the dication, 7^{2+}, isolated from a bulk two-electron chemical reduction (Cp_2Co) of 4^{4+}. It was important, therefore, to examine the electrochemical behavior of the 7^{2+} dication. The 7^{2+} dication is quite stable in dichloromethane but decomposes rapidly in donor solvents such as acetone and propylene carbonate. On the other hand, the tetracation, 4^{4+}, is completely insoluble in dichloro-

(23) Nicholson, R. S.; Shain, I. *Anal. Chem.* **1964**, *36*, 706–723.

(24) (a) Nicholson, R. S. *Anal. Chem.* **1965**, *37*, 1351–1355. (b) Nicholson, R. S. *Anal. Chem.* **1965**, *37*, 667–671.

(25) Strictly speaking, the working curve of Figure 4 refers only to Nernstein electron-transfer reactions, whereas the present Ru couples display quasi-reversible charge-transfer kinetics. However, the effect of minor changes in charge-transfer rates on the working curve, and thus on the measured rate constant k_f, is not large. The estimated life time at room temperature is based on the assumption that the first-order rate doubles for each ten-degree increase in temperature.

methane. This made it difficult to make a direct comparison between the cyclic voltammetry of 4^{4+} and that of 7^{2+}. Furthermore, the electrochemistry of this sample of 7^{2+} at potentials negative of about −0.8 V was affected by the reduction waves of Cp_2Co^+, present as a contaminant from the chemical preparation of 7^{2+} by reduction with Cp_2Co. However, a cyclic voltammogram of 7^{2+} in dichloromethane shows an anodic wave, E_p, at about +0.88 V that is 1.3 V more positive than the $E_{1/2}$ value (−0.411 V) shown by the $4^{4+}/4^{2+}$ couple!

The irreversible nature of the anodic wave of 7^{2+} is clearly due to the severe electrode precipitation of the insoluble 4^{4+} tetracation. Scanning partially through the wave led to a dissolution/desorption wave on the return sweep at about −0.7 V. This irreversible peak increased in height and shifted to more negative potential, when the scan was reversed further on the oxidation side. When the desorption peak was large, a second wave appeared at $E_{p,c} \cong -1.2$ V, which corresponds to a decomposition wave previously described for 4^{4+}. The proximity of the desorption wave to the $4^{2+}/4^0$ couple and the observation of an apparent decomposition product of 4^{4+} suggest that the oxidation of 7^{2+} at +0.88 V yields the insoluble 4^{4+} tetracation.

Reduction of the 4+ Diruthenium Complexes. Interpretation and Structural Implications. If the behavior of the paracyclophane derivative 4^{4+}, for which the evidence is most complete, is assumed to be representative of this whole group of 4+ diruthenium complexes, a reasonable interpretation of their reduction, both electrical and chemical, can be offered. Clearly, the electrochemical reduction of the 4^{4+} ion occurs by two reversible two-electron reduction steps leading to the 4^{2+} ion and then to the neutral 4^0 species.[26] At present there is no evidence to allow an exact description of either the 4^{2+} ion orthe neutral 4^0 species. Structure **23** may be equivalent to the 4^{2+} ion, but, if not, it is quite probably a closely related transient ion. A simple structural reorganization of **23** would then lead to the more stable dications **7a** and **7b**. Since either the 4^{2+} ion or **23** would be converted rapidly to **7a** and **7b** at room temperature, chemical reduction of the 4^{4+} ion provides the 7^{2+} ion directly in high yield.

The answer to the question of why the ^1H and ^{13}C NMR spectra of **7** is unsymmetrical and relatively unaffected by changing the temperature is now also apparent. Equilibration between **7a** and **7b** to give a time-averaged spectrum cannot occur directly but, instead, requires an intermediate such as **23** or the 4^{2+} ion. That the energy barrier for such an equilibration must be quite large is in accord with the assignment of the electrochemical waves of 7^{2+}, which suggest that the oxidation of 7^{2+} to 4^{4+} is at least 1 V more positive than the $4^{4+}/4^{2+}$ couple.

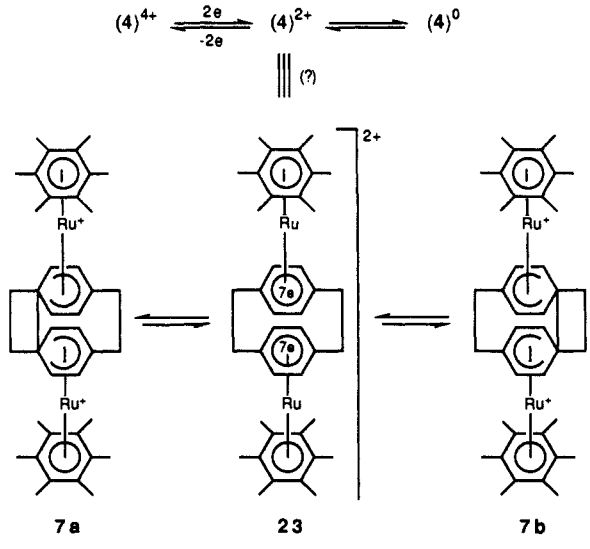

7a **23** **7b**

The important feature in the stabilization of the 2+ diruthenium ions **7**, **8**, **12**, **13**, and **14** is obviously the conversion of the benzene decks of the cyclophane moiety to two cyclohexadienyl anion decks joined by a carbon–carbon bond. Steric strain should play an important role in whether such a phenomenon occurs. For that reason it was of interest to study the 4+ diruthenium complexes of the multibridged cyclophanes, [2₅](1,2,3,4,5)cyclophane[27] and [2₆](1,2,3,4,5,6)cyclophane (superphane).[28,29] The extreme rigidity of these multibridged cyclophanes would suggest that their conversion to a cyclophane with cyclohexadienyl anion decks joined by a carbon–carbon bond would be extremely difficult, if not impossible.

Following the same general procedures used previously, we were able to prepare the 4+ diruthenium complexes **24** and **25** readily and in good yield. Cyclic voltammetry of **24** showed a partially reversible two-electron reduction wave ($E_{1/2}$ = −0.413 V). However, attempts to carry out a two-electron chemical reduction of **24** and isolate the corresponding 2+ ion were unsuccessful, yielding no useful product. In the case of **25**, though, cyclic voltammetry showed two reversible one-electron reduction waves ($E_{1/2}$ = −0.583 V; $E'_{1/2}$ = −0.760 V). But again, attempted chemical reduction experiments to give the corresponding 2+ or 3+ ions led to no useful product. Despite the fact that the reduction products of these multibridged 4+ diruthenium-cyclophane complexes are apparently very unstable, the cyclic voltammetry of **25** does suggest that the very rigid geometry of superphane does not permit the special stabilization on two-electron reduction that is observed for 4^{4+} and the other more flexible cyclophane ligands.

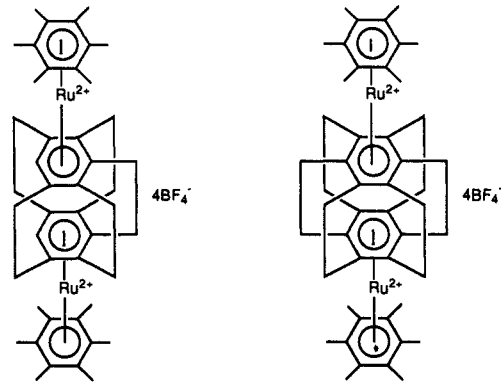

24 **25**

Theoretical Description of the Molecular and Electronic Structures of 2, 7, 8, 12, 13, and 14. The essential point which must be addressed concerns the differences in the two-electron reductive behavior between **1** and the new compounds **4**, **5**, **9**, **10**, and **11**. Whereas the site of reduction of **1** was shown to be one of the ruthenium atoms (to produce **2**), in the case of the latter compounds reduction occurs exclusively at the cyclophane ligand, leaving both of the ruthenium atoms in 2+ oxidation states. Given the fact that it is this latter mode of reduction which predominates we shall begin by focusing on these reduction products.

In each complex we have a pair of benzene rings held in a particular geometry by the cyclophane linkages, which serve as the reservoir for the additional pair of electrons. The lowest unoccupied molecular orbitals (LUMO) are degenerate, (e_{2u}) in benzene, and are shown in real form below.

S **A**

Irrespective of which orbitals become populated, the simple addition of two electrons to the pair of benzene rings forces each

(26) Recently (Pierce, D. T.; Geiger, W. E. *J. Am. Chem. Soc.* **1989**, *111*, 7636–7638), it has been shown that the two-electron reduction of (η^6-C_6Me_6)Ru^{2+} occurs by two, one-electron steps. Quite probably, each of these two-electron reduction steps, $(4)^{4+} \rightarrow (4)^{2+} \rightarrow (4)^0$, may also be two, one-electron steps.

(27) Schirch, P. F. T.; Boekelheide, V. *J. Am. Chem. Soc.* **1981**, *103*, 6873–6878.
(28) Sekine, Y.; Boekelheide, V. *J. Am. Chem. Soc.* **1981**, *103*, 1777–1785.
(29) Hanson, A. W.; Cameron, T. S. *J. Chem. Res.* **1980**, 336–337.

Ru(II) to complex with a formally 7π-ligand which would exceed the favored electron count around the rutheniums. A solution to this problem is illustrated below for the *anti*-[2$_2$](1,3)cyclophane moiety present in the case of **8**. By placing the two electrons in the symmetric pair of orbitals it is clear that the structure may smoothly transform into the bis(cyclohexadienyl) geometry. This absorbs the extra pair of electrons into the transannular σ-bond and retains the favored electron count around ruthenium. Inspection of the orbitals involved shows this process to be symmetry allowed.

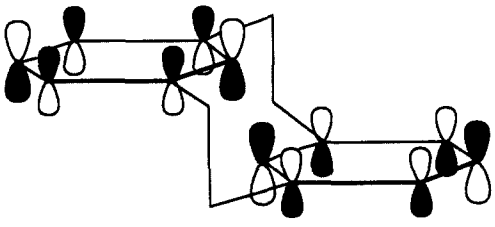

It is well-known that *anti*-[2$_2$](1,3)cyclophanes readily undergo C4–C12 bond formation during chemical reactions, such as oxidation[19] or electrophilic substitution.[20] Thus, C4–C12 bond formation should be an easy process in the case of **8**, and the C4–C12 bond length should not be much longer than a normal sp^3–sp^3 bond. Although anionic dimerizations are unprecedented in cyclophane chemistry, there are two comlexes of tetracyanoquinodimethane (TCNQ) anions which are known to undergo intermolecular σ-bond formation at the exocyclic methylene groups in the solid state. Bis(dipyridyl)platinum(II)–TCNQ[30] shows a σ-bond length of 1.65 Å between TCNQ pairs, whereas in *N*-ethylphenazenium–TCNQ[31] the bond distance is 1.63 Å. In both cases the TCNQ dimers adopt an extended configuration, so that the benzenoid fragments of the molecules are *not* superimposed (analogous to **8**, as illustrated above).

The crystal structure of **7** shows that bonding in this compound is considerably more complicated, and the same remarks probably also apply to the other complexes which contain the [2$_2$](1,4)-cyclophane ligand (**12** and **13**). These complexes also make use of the symmetric LUMO as shown below. The transformation between the two different bis(cyclohexadienyl) structures is still symmetry allowed, and it is only the propensity of the Ru(II) atoms for 6π-ligands which inhibits the occurrence of this rearrangement.

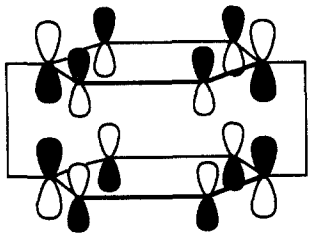

It appears that the structure exhibited by **7** represents a compromise between the preference of the rutheniums for complexation with a 6π-ligand, which forces the formation of a *single* σ-bond, and the natural desire of the reduced benzene moieties to distribute the electron density symmetrically and so equalize the bonding between decks at the 3(14) and 6(11) positions. The final structure exhibits the distortional characteristics of a second-order Jahn–Teller effect in which the electron density has shifted, but certain aspects of the symmetrical molecular structure still remain.

This latter point is made clear in the analyses of the crystal structure of **7** presented in Tables V and VI. The π-orbital axis vector (POAV) analysis[32,33] shows that C3 and C14, and to a lesser extent C6 and C11, are significantly pyramidalized (for a tetrahedral carbon $\theta_{\sigma\pi}$ = 109.47°). Similarly, the π-orbital of these carbons shows evidence of rehybridization from pure p toward sp^3 (s$^{1/3}$p in the present notation). Nevertheless these values are exceeded in certain (stable) alkenes, and it is clear that a substantial degree of π-bonding is maintained within the benzene rings even at C6 and C11. This point is supported by the cyclohexadienyl ring bond lengths, which have the average values shown below.

Table V. POAV Analysis of the Crystal Structure of **7**

atom	POAV1 $\theta_{\sigma\pi}$ (deg)	POAV2 m (s^{m}p)
C3	101.64	0.0878
C14	99.69	0.0611
C6	93.08	0.0056
C11	90.99	0.0006

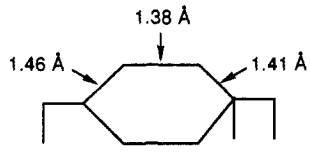

The feature which clearly differentiates **7** from **8** is made obvious in the 3D-HMO analysis,[33,34a] presented in Table VI, where it may be seen that there is not only bonding between the C3–C14 pair but also a strong interaction between the C6–C11 atoms. The ρ_B value between the C6–C11 pair is more than 50% of that between the C3–C14 atoms. The strength of both of these interactions is partly attributable to the *sense* of the π-orbital axis vectors (POAV) at these carbon atoms. In every case the POAV is directed toward the bonding partner. This point is made clear in Figure 2, where it may be seen that the rehybridization is such that the s-character mixes into the p-orbital so that bonding between decks is reinforced. This provides clear evidence of a favorable interaction and is most unusual for a cyclophane. In superphane, for example, the POAVs are directed away from the opposite deck, and the significant pyramidalization ($\theta_{\sigma\pi}$ = 96.58°) serves to reduce the ρ_B to 0.297.[34b] It is interesting to note that the interaction between decks is almost purely of σ-character which implies that the POAV hybrids point directly toward the bonding partner. To some extent this is dictated by the geometry, however, and is quite common in the cyclophanes. It would be of some interest to examine the interactions between the other pairs of carbons and within the benzene rings, but without the coordinates of the hydrogen atoms this is not possible in POAV theory.

On the basis of the evidence presented above we believe that **7**, **12**, and **13** provide support for the existence of a new bonding principle in which there is self-complexation between anionic π-systems, and on this basis we shall refer to this electronic structure as a π$^-$,π$^-$-complex.

Finally, we turn to the reduction of **1** in which the cyclophane ligand does not accept the added pair of electrons. The two possible LUMOs for population in the reduction product of this cyclophane are shown below, and it is clear that the interactions induced by placing the electrons in the symmetric (S) orbital would introduce considerable strain as it requires the close approach of all six pairs of carbon atoms. The electrochemistry of **24** and **25** shows this to be an unfavorable situation. This leaves the antisymmetric (A) LUMO which has equal coefficients at four carbon atoms and therefore offers no unique position for formation of a σ-bond between decks. Furthermore, it can be shown that the conversion of this orbital into the requisite cyclohexadienyl structure is symmetry forbidden.

In the case of **1**, the formation of **2** provides an alternate pathway for which the geometry of **1** is very favorable. As shown by X-ray analysis,[35] the benzene decks of **1** are boat-shaped with

(30) Dong, V.; Endres, H.; Keller, H. J.; Moroni, W.; Nothe, D. *Acta Crystallogr.* **1977**, *B33*, 2428–2431.
(31) Morosin, B.; Plastas, H. J.; Coleman, L. B.; Stewart, J. M. *Acta Crystallogr.* **1978**, *B34*, 540–543.
(32) Haddon, R. C. *J. Am. Chem. Soc.* **1986**, *108*, 2837–2842.
(33) Haddon, R. C. *Acc. Chem. Res.* **1988**, *21*, 243–249.
(34) (a) Haddon, R. C. *J. Am. Chem. Soc.* **1987**, *109*, 1676–1685. (b) Haddon, R. C. To be published.

the prow and stern of the boats directed away from the center of the molecule. Thus, there is very little change in the geometry of the cyclophane as a Ru(II) atom of δ^6-hapticity changes to a Ru(0) atom with η^4-hapticity.

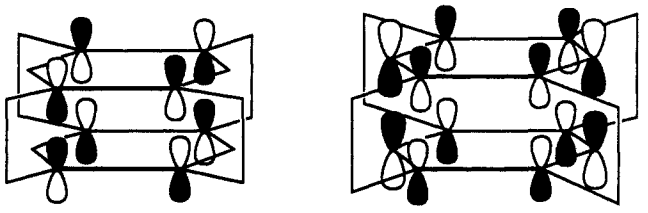

A S

In conclusion, the important finding of this study is that the general behavior of 4+ diruthenium–cyclophane complexes on two-electron reduction is the formation of cyclophane ligands having two cyclohexadienyl anion decks connected by a carbon–carbon bond. The fact that ruthenium–cyclophane complexes with cyclohexadienyl anion decks can readily be prepared raises the possibility of interesting applications for this class of molecules. For some time we have been concerned with potential polymers based on cyclophane–transition-metal complexes, whose mixed-valence ion character might provide interesting magnetic or electrical properties.[2] In a related theoretical study,[36] Burdett and Canadell have pointed out that a stacked, columnar polymer, based on metallocene monomer units, should have interest as a potential electrical conductor. Kasahara et al.[37] and Jutzi et al.[38] have prepared dimetal complexes of $[3_2]$- and $[4_2](1,3)$cyclopentadienylophanes, but the distance between decks in these metallocenes is too great to allow an appreciable interaction between the two attached metal atoms.

The short distance between the cyclohexadienyl anion decks of **7** and the strong interaction evident between the two ruthenium atoms, though, makes the possibility of preparing a stacked, metallocene polymer based on monomer units of this type an extremely attractive goal. First of all, the solvated ruthenium complex of paracyclophane, **26**, is readily available,[3] and its conversion to a metallocene polymer, such as **27**, by electrochemical crystal growth seems quite feasible. The probable air stability of **27** and its likely solubility in nonpolar organic solvents are also of practical interest. Finally, an extended Hückel calculation of the tetramer corresponding to **27** indicates its bonding HOMO is delocalized over all of the ruthenium atoms and cyclophane units.[39]

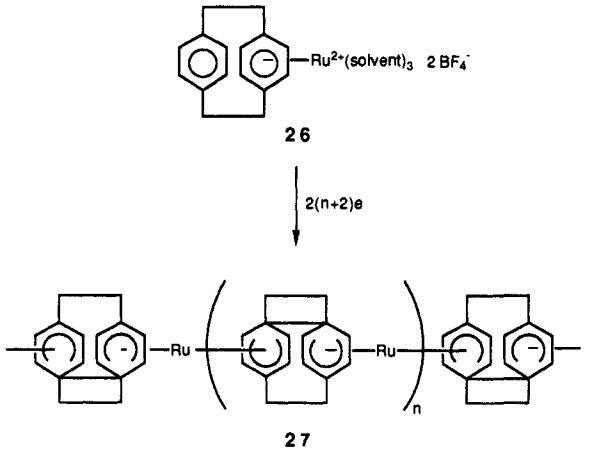

(35) Hanson, A. W. *Acta Crystallogr., Sect. B* **1977**, *33*, 2003–2007.
(36) Burdett, J. K.; Canadell, E. *Organometallics* **1985**, *4*, 805–815.
(37) Kasahara, A.; Izumi, T.; Yoshida, Y.; Shimizu, I. *Bull. Chem. Soc. Jpn.* **1982**, *55*, 1901.
(38) Jutzi, P.; Siemeling, U.; Müller, A.; Bögge, H. *Organometallics* **1989**, *8*, 1744–1750.
(39) Private communication from Prof. C. E. Klopfenstein and Dr. G. Purvis. The extended Hückel calculations were made by using a CACHE program.

Table VI. POAV2/3D-HMO Analysis of the Crystal Structure of **7**

atoms	ρ^{B}[a]	character[b] σ	character[b] π
C3–C14	1.345	0.969	0.031
C6–C11	0.693	0.978	0.022

[a] Reduced resonance integral as a fraction of the benzene resonance integral (β). [b] With respect to the axis between the pair of atoms.

Experimental Section[40]

Bis(η^6-hexamethylbenzene)(η^6,η^6-[2_2](1,4)cyclophane)diruthenium-(II,II) Tetrakis(tetrafluoroborate) (4). Model Procedure for Bis Capping. A mixture of 1.54 g (4.62 mmol) of bis(hexamethylbenzene)dichlorobis(μ-chloro)diruthenium(II)[43] and 1.799 g (9.24 mmol) of silver tetrafluoroborate in 20 mL of acetone was stirred at room temperature for 30 min. The resulting precipitate of silver chloride was collected by filtration and washed with acetone until the washings were clear and colorless. After concentration of the combined filtrate and washings almost to dryness, 96.2 mg (0.462 mmol) of [2_2](1,4)cyclophane and 5 mL of trifluoroacetate acid were added to the residue. The mixture was then boiled under reflux for 2 h. After the mixture had cooled, the resulting precipitate was collected by filtration and washed with acetone. The yellowish white solid remaining on the filter was dissolved in nitromethane and then reprecipitated by addition of ether. The resulting solid was again collected by filtration, washed with a small amount of acetone, and dried to give 490 mg (98%) of **4** as a pale yellow solid, identical in all respects with a sample previously prepared.[6]

(40) All reactions with air-sensitive compounds were conducted either in a Vacuum Atmospheres Co. double-length drybox (Model HE-553-2 Dri-Lab) or in Schlenk-Ware. All NMR spectra were measured on a General Electric QE-300 (300 MHz) system or a Nicolet NT-360 spectrometer. Ultraviolet spectra were recorded on a Beckman DU-7 and infrared spectra with a Beckman IR 4240 spetrometer. Melting points were determined in sealed, evacuated capillary tubes on a Mel-Temp apparatus and are uncorrected. Elemental analyses were performed by Desert Analytics or Schwarzkopf Microanalytical Laboratory. In the electrochemical procedures all cyclic voltammetry (CV) were carried out under nitrogen in a Vacuum Atmospheres Co. drybox by using a Princeton Applied Research (PAR) Model 173 potentiostat equipped with a Model 179 coulometer/current-to-voltage converter and a Model 175 voltage function programmer. Variable temperature experiments (±1 °C) were carried out with the cell partially immersed in a heptane bath cooled by a Flexi-cool coil (FTS Systems Inc.). Voltammetric waveforms below $v = 0.5$ V s^{-1} were recorded on a Hewlett-Packard 7046B X-Y recorder. Otherwise all data were acquired and stored on a Nicolet 4094 digital oscilloscope (Nicolet Instrument Co., Madison, WI) equipped with a Model 4175 8-bit plugin and Model F-43/2 dual disk recorder. Signal averaging of 5–20 CV scans per scan recorded was afforded by the Model 4175 plugin. Digitized scans were transferred to an AT&T personal computer 6300 (AT&T Consumer Products, King of Prussia, PA) for subsequent processing and display. Voltammetry was performed in acetone, propylene carbonate, or dichloromethane with n-Bu_4NPF_6 (0.1 M) as supporting electrolyte. A three-electrode cell configuration was employed with a platinum wire auxiliary electrode in solution and a solid silver/silver chloride or saturated calomel (SCE) reference electrode isolated from solution by a fine glass frit within a luggin capillary probe. Ferrocene (Fc) was introduced as an internal reference standard at the conclusion of each experiment. CV experiments were performed at HMDE, Pt bead, or Pt microdisk electrodes, all potentials were referenced to the Fc/Fc^+ couple for the particular media, and temperatures were reported. Potentials were converted to SCE scale at 298 K by addition of +0.48 V (acetone), +0.46 V (dichloromethane), or +0.37 V (propylene carbonate). Effects due to solvation resistance at the working electrode were minimized for high sweep rate CV scans (above ca. 1.0 V s^{-1}) by using the smallest working electrode possible without introducing appreciable radial diffusion and by employing positive feedback compensation afforded by the PAR 179.[41] The most efficient compensation was achieved by shunting a second platinum wire in solution to the reference electrode with a 0.1 μF capacitor.[42] When possible, charging current was subtracted from high sweep rate CV scans by recording matching waveforms before and after addition(s) of analyte. The matching background and analyte scans were subtracted point-by-point and smoothed by using an 11-point polynomial smoothing routine (Savitsky, A.; Golay, M. *J. Anal. Chem.* **1969**, *36*, 1627) on the AT&T PC 6300. Computer simulations of CV waveforms as described by Feldberg (Feldberg, S. W. *Electroanal. Chem.* **1969**, *3*, 199) were executed on the AT&T PC 6300 by using the Microsoft FORTRAN Optimizing Compiler (version 4.0, Microsoft, Redmond, WA).

(41) (a) Radial diffusion contribution to the overall current was calculated to beless than 3% at Pt disk electrode ($r_o = 238$ μM) and HMDE ($r_o > 250$ μM) at $v = 1.0$ V s^{-1}. (b) Heinze, J. *Ber. Bunsen-Ges. Phys. Chem.* **1981**, *85*, 1096–1103.
(42) Garreau, D.; Saveant, J. M.; Binh, S. K. *J. Electroanal. Chem.* **1978**, *89*, 427.
(43) Bennett, M. A.; Matheson, T. W.; Robertson, G. B.; Smith, A. K.; Tucker, P. A. *Inorg. Chem.* **1980**, *19*, 1014–1021.

Compounds **9**, **10**, **11**, **16**, and **25** were prepared similarly following this procedure. See the Supplementary Material section for experimental details.

Bis(η^6-hexamethylbenzene)(η^5,η^5-[2$_2$](1,4)cyclophane)diruthenium-(II,II) Bis(tetrafluoroborate) (7). Model Chemical Reduction Procedures with Cobaltocene. A mixture of 316.9 mg (0.293 mmol) of **4** and 110.7 mg (0.586 mmol) of cobaltocene in 12 mL of methanol was stirred at room temperature for 2.5 h under an inert atmosphere. After concentration of the greenish-yellow mixture, the residue was washed into a thimble and then placed in a Schlenk-Soxhlet apparatus, where it was extracted with 1,2-dimethoxyethane for 48 h to remove the cobaltocenium tetrafluoroborate. The remaining contents in the thimble consisted of 225.4 mg (85%) of **7** as a reddish brown solid. Recrystallization of this by solution in dichloromethane followed by a slow vapor diffusion of ether afforded small red crystals: mp > 280 °C dec; ^{1}H and ^{13}C NMR data (see Table II).

Compounds **12** and **13** were likewise prepared following this procedure. See the Supplementary Material section for experimental details.

Bis(η^6-hexamethylbenzene)(η^5,η^5-*anti*-[2$_2$](1,3)cyclophane)diruthenium(II,II) Bis(tetrafluoroborate) (8). Model Chemical Reduction Procedure with Bis(hexamethylbenzene)ruthenium(0). A mixture of 100 mg (0.092 mmol) of **5**[13] and 39 mg (0.092 mmol) of bis(hexamethylbenzene)ruthenium)(0)[13] in 7 mL of methanol was stirred at room temperature for 20 h under an inert atmosphere. After removal of solvent by concentration, the residue was taken up in dichloromethane, and this solution was filtered to remove insoluble residues. Concentration of the filtrate followed by crystallization of the residue from dichloromethane subjected to slow vapor diffusion with acetone gave 70 mg (83%) of a red solid. When the reduction was repeated by using the model cobaltocene procedure previously described for **7**, the product was identical and, again, was isolated in 83% yield as red crystals: mp >200 °C dec; ^{1}H and ^{13}C NMR (see Table II); λ_{max} (CH_2Cl_2) 391.5 (ϵ, 7800) and 325.5 nm (ϵ, 8700); λ_{max} (CH_3OH) 385 (ϵ, 10 700) and 322 nm (ϵ, 12 600). Anal. Calcd for $C_{40}H_{52}Ru_2B_2F_8 \cdot CH_2Cl_2$: C, 49.57; H, 5.27. Found: C, 49.17; H, 5.55. The presence of a molecule of dichloromethane of crystallization was confirmed by an X-ray analysis.[46]

Compound **14** was likewise prepared following this procedure. See the Supplementary Materials section for experimental details.

Acknowledgment. We thank the National Science Foundation for their support of this investigation under Grants CHE-8709775 and CHE-8603728. K.-D.P. thanks the Studienstiftung des Deutschen Volkes for a Discussion Stipend (1985-1987).

Supplementary Material Available: Tables of atomic coordinates and interatomic distances and bond angles derived from the crystallographic analysis of **7** and a detailed experimental section (30 pages); tables of observed and calculated structure factors (21 pages). Ordering information is given on any current masthead page.

(44) Rohrbach, W. D.; Boekelheide, V. *J. Org. Chem.* **1983**, *48*, 3673-3678.

(45) Boekelheide, V.; Hollins, R. A. *J. Am. Chem. Soc.* **1972**, *95*, 3201-3208.

(46) An X-ray analysis of **8**, carried out by Oneida Research Services, confirmed the presence of a molecule of dichloromethane of crystallization. We thank Dr. Michael D. Ward and E. I. du Pont de Nemours & Co. for providing this service.

Bis(η^6-hexamethylbenzene)(η^6,η^6-polycyclic aromatic)diruthenium(II,II) Complexes and Their Two-Electron Reduction to Cyclohexadienyl Anion Complexes[1]

Klaus-Dieter Plitzko, Gabriele Wehrle, Bernhard Gollas, Brian Rapko, Jörg Dannheim, and Virgil Boekelheide*

Contribution from the Department of Chemistry, University of Oregon, Eugene, Oregon 97403.
Received January 8, 1990

Abstract: The bis(η^6-hexamethylbenzene)(η^6,η^6-polycyclic aromatic)diruthenium(II,II) complexes **10**, **14**, **16**, **18**, **20**, and **22**, where the polycyclic aromatic ligands are phenanthrene, 9,10-dihydrophenanthrene, biphenyl, 3,3',5,5'-tetramethylbiphenyl, 4,5,9,10-tetrahydropyrene, and triphenylene, respectively, have been synthesized and their electrochemical properties measured. A two-electron chemical reduction of each of these 4+ diruthenium complexes has led to the isolation and characterization of each of their corresponding 2+ diruthenium complexes: **11**, **15**, **17**, **19**, **21**, and **23**. On the basis of analyses of their ^{1}H and ^{13}C NMR spectra, structural assignments have been made for all of these 2+ diruthenium complexes. Although the phenanthrene derivative **11** is a class II mixed-valence ion having a Ru(0) site and a Ru(II) site, all of the other 4+ diruthenium complexes undergo two-electron reduction by changing the biphenyl moiety of their polycyclic aromatic ligand into two cyclohexadienyl anions joined by a carbon-carbon double bond. That the bis(cyclohexadienyl anion) system present in these 2+ diruthenium complexes is subject to electrophilic attack was shown by the easy protonation of **17**, leading to the formation of **37**. The 4+ diruthenium complex of biphenylene **42** was prepared, and it undergoes a similar two-electron reduction to give **43**. In contrast, though, the highly rigid 4+ diruthenium complex of pyrene **35** shows two separate one-electron reduction waves. The bis(η^6-biphenyl)ruthenium(II) bis(tetrafluoroborate) derivatives **49**, **50**, and **51** were prepared. A single-crystal X-ray analysis of **49** shows the molecule to have a syn conformation.

The possibility that polymers derived from transition-metal complexes of [2$_n$]cyclophanes might show interesting electrical properties associated with electron delocalization has led us to prepare various model monomers related to such polymers and examine their properties.[2-4] [2$_n$]Cyclophanes are attractive ligands because their π-electron systems are delocalized, yet they present two arene decks for metal complexation, as is necessary for polymer formation. Another class of compounds offering π-electron delocalization combined with two sites for metal com-

(1) Preliminary communication: Plitzko, K.-D.; Boekelheide, V. *Angew. Chem.* **1987**, *99*, 715-717; *Angew. Chem., Int. Ed. Engl.* **1987**, *26*, 700-702.

(2) Laganis, E. D.; Finke, R. G.; Boekelheide, V. *Tetrahedron Lett.* **1980**, *21*, 4405-4408.

(3) Voegeli, R. H.; Kang, H. C.; Finke, R. G.; Boekelheide, V. *J. Am. Chem. Soc.* **1986**, *108*, 7010-7016.

(4) Plitzko, K.-D.; Rapko, B.; Gollas, B.; Wehrle, G.; Weakley, T.; Pierce, D.; Geiger, W. E., Jr.; Haddon, R. C.; Boekelheide, V. *J. Am. Chem. Soc.* **1989**, *111*, XXXX.

0002-7863/90/1512-6556$02.50/0